Glycobiology vol. 9 no. 1 pp. 21–30, 1999

Glycosylation sites and site-specific glycosylation in human Tamm-Horsfall glycoprotein

Johannes J.M.van Rooijen, Anton F.Voskamp, Johannis P.Kamerling and Johannes F.G.Vliegenthart[1]

Bijvoet Center, Department of Bio-Organic Chemistry, Utrecht University, P.O. Box 80075, NL-3508 TB Utrecht, The Netherlands

Received on March 2, 1998; revised on May 15, 1998; accepted on May 25, 1998

[1]To whom correspondence should be addressed

The N-glycosylation sites of human Tamm-Horsfall glycoprotein from one healthy male donor have been characterized, based on an approach using endoproteinase Glu-C (V-8 protease, *Staphylococcus aureus*) digestion and a combination of chromatographic techniques, automated Edman sequencing, and fast atom bombardment mass spectrometry. Seven out of the eight potential N-glycosylation sites, namely, Asn52, Asn56, Asn208, Asn251, Asn298, Asn372, and Asn489, turned out to be glycosylated, and the potential glycosylation site at Asn14, being close to the N-terminus, is not used. The carbohydrate microheterogeneity on three of the glycosylation sites was studied in more detail by high-pH anion-exchange chromatographic profiling and 500 MHz ^{1}H-NMR spectroscopy. Glycosylation site Asn489 contains mainly di- and tri-charged oligosaccharides which comprise, among others, the GalNAc4*S*(β1–4)GlcNAc terminal sequence. Only glycosylation site Asn251 bears oligomannose-type carbohydrate chains ranging from $Man_5GlcNAc_2$ to $Man_8GlcNAc_2$, in addition to a small amount of complex-type structures. Profiling of the carbohydrate moieties of Asn208 indicates a large heterogeneity, similar to that established for native human Tamm-Horsfall glycoprotein, namely, multiply charged complex-type carbohydrate structures, terminated by sulfate groups, sialic acid residues, and/or the Sd^a-determinant.

Key words: Tamm-Horsfall glycoprotein/carbohydrate/NMR/site-specific glycosylation

Introduction

Human Tamm-Horsfall glycoprotein (THp) is the most abundant protein in normal human urine, being excreted in quantities of up to 100 mg/day (Tamm and Horsfall, 1950; Tamm and Horsfall, 1952). THp is produced by the kidney where it is expressed via a phosphatidylinositol anchor on the endothelium of the thick ascending limb of the loop of Henle (Sikri *et al*., 1979; Rindler *et al*., 1990). The physiological function of THp is still controversial. THp could act as a natural inhibitor of microbial infection of the urinary tract and urinary bladder (Duncan, 1988; Parkkinen *et al*., 1988). A possible relation between THp and the electrolyte/water transport in the nephron has been described previously (Mattey and Naftalin, 1992) as well as a role in the formation of kidney stones (Hallson and Rose, 1979; Scurr and Robertson, 1986). The ability to inhibit antigen-specific T-cell proliferation *in vitro* probably due to the glycan part of the protein has been reported but the results are ambiguous (Muchmore *et al*., 1987; Moonen *et al*., 1988). Furthermore, the carbohydrate chains of THp have been implicated in the binding to neutrophils (Toma *et al*., 1994) and in immunosuppressive properties (Sathyamoorthy *et al*., 1991).

In earlier studies, it has been found that THp built up from a polypeptide backbone of 616 amino acids, has a carbohydrate content of 25–30% (w/w) (Kumar and Muchmore, 1990), distributed over eight potential N-glycosylation sites, Asn14, Asn52, Asn56, Asn208, Asn251, Asn298, Asn372, and Asn489 (Hession *et al*., 1987; Pennica *et al*., 1987), of which at least five are occupied (Afonso *et al*., 1981). So far, no data have been reported about the specific asparagine residues involved in the glycosylation, nor about the heterogeneity of the carbohydrate chains at each occupied glycosylation site.

Detailed structural studies of the total glycosylation pattern of THp from individual male donors have resulted in the elucidation of 63 complex-type N-glycans, which form only part of the 150 isolated carbohydrate-containing fractions (Hård *et al*., 1992; van Rooijen *et al*., 1998a, b; see also Donald *et al*., 1983; Serafini-Cessi *et al*., 1984b; Williams *et al*., 1984; Donald and Feeney, 1986). Di-, tri-, and, most of all, tetraantennary structures (including dimeric *N*-acetyllactosamine sequences) are present which can be fucosylated, sialylated (including the Sd^a-determinant) and/or sulfated. Furthermore, oligomannose-type carbohydrate chains are reported for THp from pooled urine of various individuals ranging from $Man_5GlcNAc_2$ to $Man_7GlcNAc_2$ (Serafini-Cessi *et al*., 1984a; Dall'Olio *et al*., 1988; Smagula *et al*., 1990).

In this study, a detailed analysis of the glycosylation sites of THp is presented in order to contribute to the unraveling of the biological functions of human THp.

Results

THp (100 mg) was isolated from 2 l morning urine from a healthy male donor. It was checked for purity by SDS–PAGE, demonstrating a single band at 94 kDa under reducing conditions. Monosaccharide analysis of THp revealed the presence of Fuc, Man, Gal, GalNAc, GlcNAc, and Neu5Ac in a molar ratio of 0.9:3.0:3.7:1.1:5.5:2.9, and the carbohydrate content was found to be 28% by mass. In order to generate information with respect to glycosylation sites and site-specific glycosylations in THp, the analysis strategy as depicted in Figure 1 has been followed. The amino acid sequence of human THp has been published before (Hession *et al*., 1987; Pennica *et al*., 1987) and is shown in Figure 2.

After reduction and *S*-carboxymethylation, THp (50 mg) was incubated with endoproteinase Glu-C (V-8 protease), and the progress of digestion was followed by HPLC on ChromSpher 5 C8. Gel permeation chromatography on HiTrap of the digest

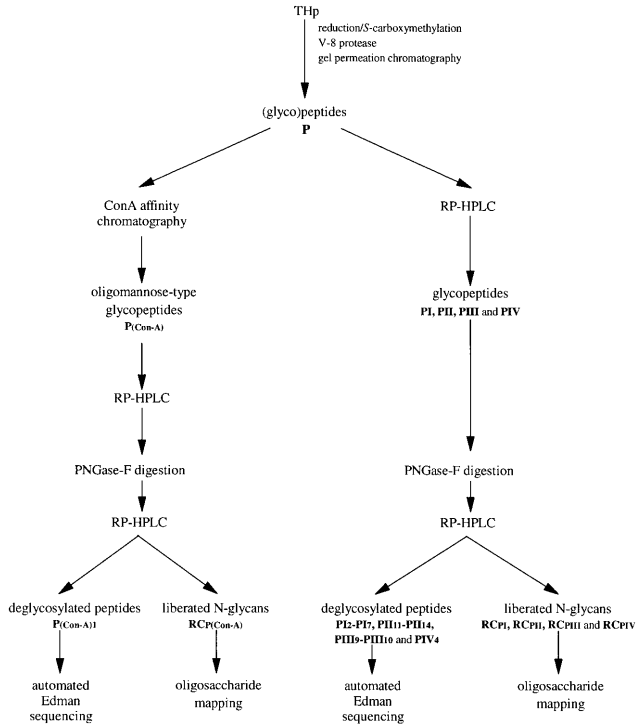

Fig. 1. Work-up procedure for the V-8-protease digest of reduced and *S*-carboxymethylated THp.

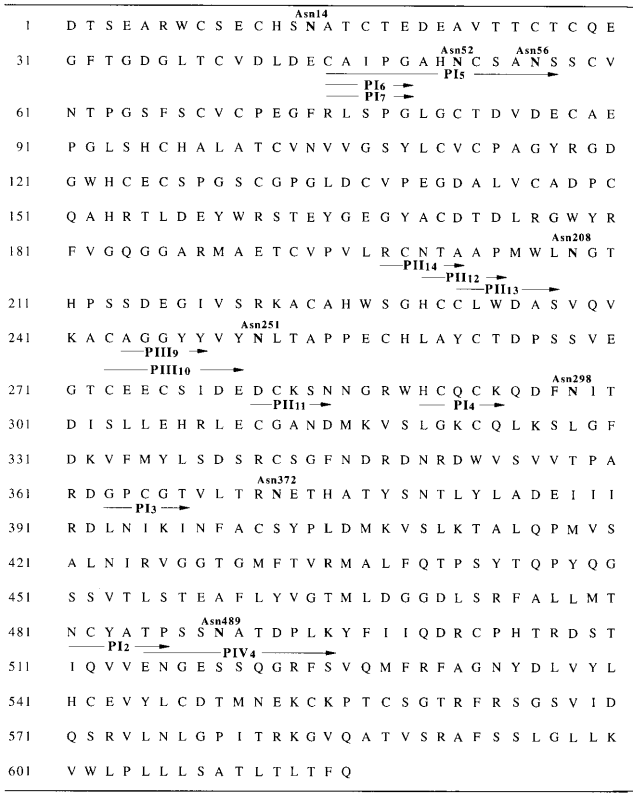

Fig. 2. The amino acid sequence of THp, as deduced from cDNA and chemical sequencing (Hession *et al*., 1987; Pennica *et al*., 1987). The Asn residues of the potential N-glycosylation sites are written in boldface type. Arrow through **PII12** represents the N-terminal amino acid sequence of peptide **PII12** generated by PNGase-F treatment of glycopeptide fraction **PII**.

afforded fraction **P**, containing the high-molecular-mass (glyco)peptides. This fraction was subjected to HPLC on ChromSpher 5 C8 (Figure 3), and the glycopeptide-containing fractions were detected by orcinol/H_2SO_4, and denoted **PI-PIV**.

In order to characterize which of the potential glycosylation sites are glycosylated, fractions **PI**, **PII**, **PIII**, and **PIV** were each treated with PNGase-F and then separated by HPLC on ChromSpher 5 C8 (Figure 4a–d). The deglycosylated peptides, denoted **PI2-PI7**, **PII11-PII14**, **PIII9-PIII10**, and **PIV4**, were subjected to amino acid sequence analysis for at least five N-terminal amino acids (Diagram II). The liberated N-glycan fractions, **RCPI**, **RCPII**, **RCPIII**, and **RCPIV**, were analyzed by 500 MHz ^{1}H-NMR spectroscopy (Figure 5a–d), in conjunction with profiling by HPAEC on CarboPac PA-100 (Figure 6b–e). In connection with the HPAEC profiling, in Figure 6a the fractionation of the total pool of N-glycans released by PNGase-F from fraction **P** is depicted. Here, the assignment of the regions differing in charge, **Q0-Q7**, is based on a sequential Resource Q-CarboPac PA-100 approach (Hermentin *et al*., 1996). Using the defined regions in Figure 6a, it is possible to identify the regions differing in charge (charge fractions) as indicated in Figure 6b–e. Ratios in percentage of different charge fractions of the carbohydrate pool of fractions **RCPI-RCPIV**, and fraction **P** itself are displayed in Figure 7.

Fraction **PIV** (Figure 4d). Peptide fraction **PIV4** was subjected to N-terminal amino acid sequence analysis affording the partial sequence T-P-X-X-X-A-T-D-P-L-K-. As is evident from Figure 2, this sequence represents Thr485-Lys495, containing Asn489 as glycosylation site. This glycosylation site is mainly substituted with di- and tri-charged oligosaccharides as concluded from the HPAEC profile of **RCPIV** (Figures 6e, 7d). ^{1}H-NMR analysis of **RCPIV** (Figure 5d) showed the presence of the Gal-NAc4*S*(β1–4)GlcNAc(β1–2)Man(α1–3)- element in the

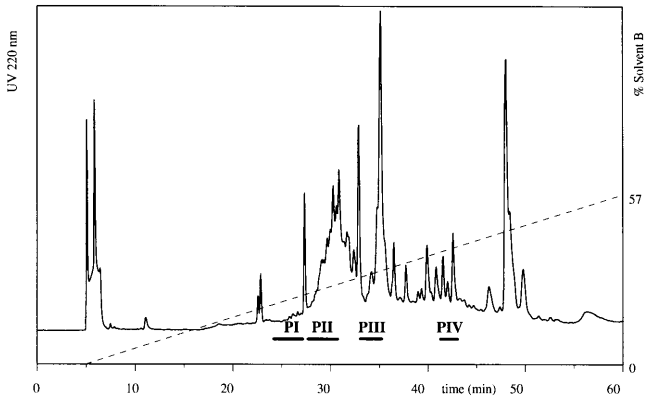

Fig. 3. Fractionation pattern at 220 nm on ChromSpher 5 C8 of (glyco)peptide fraction **P**. The elution was carried out on a ChromSpher 5 C8 column (10 × 250 mm, Chrompack), at a flow rate of 2.5 ml/min. The column was eluted isocratically with solvent A (aqueous 5% acetonitrile containing 0.1% trifluoroacetic acid) for 5 min, followed by a linear concentration gradient from 100% solvent A/0% solvent B (aqueous 80% acetonitrile containing 0.1% trifluoroacetic acid) to 43% solvent A/57% solvent B in 55 min.

carbohydrate moiety, as deduced from the structural-reporter-group signals of GalNAc (H-1, δ 4.586; H-4, δ 4.692; NAc, δ 2.069) (Hård *et al*., 1992; van Rooijen *et al*., 1998b). Furthermore, the Gal3*S* residue (H-3, δ 4.34; H-4, δ 4.29) (Kamerling *et*

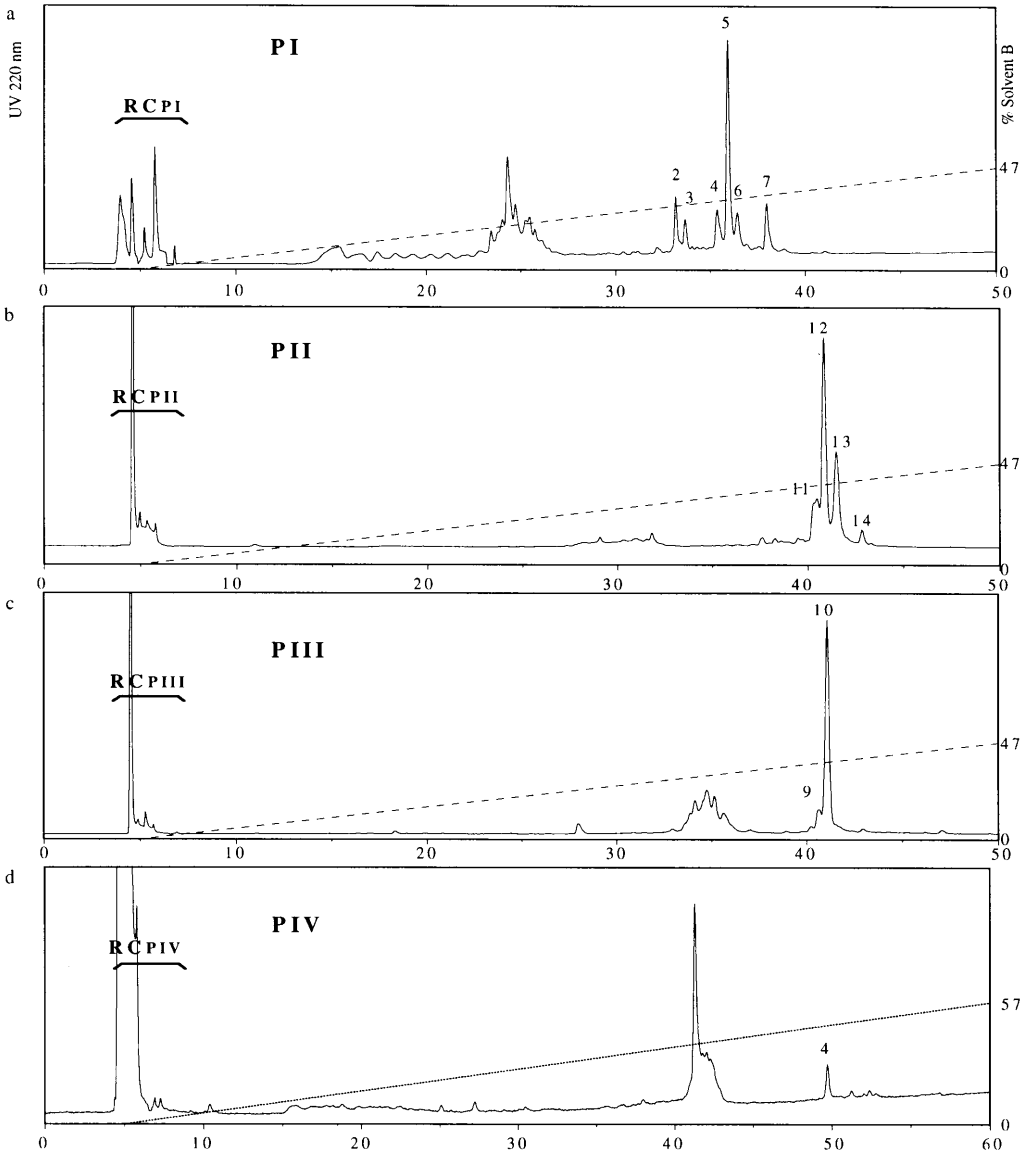

Fig. 4. Elution profiles of PNGase-F-treated glycopeptide fractions isolated from fraction **P**. (**a**) fraction **PI**, (**b**) fraction **PII**, (**c**) fraction **PIII**, and (**d**) fraction **PIV**. Elutions were performed as described in Figure 3. Fraction **RCPI, RCPII, RCPIII**, and **RCPIV** contain the carbohydrate chains liberated from the peptide fractions **PI2-PI7**, **PII11-PII14**, **PIII9-PIII10**, and **PIV4**, respectively.

al., 1988; Hård *et al*., 1992; van Rooijen *et al*., 1998b), the Sd^a-determinant (Neu5Ac H-3a, δ 1.927 and H-3e, δ 2.662; GalNAc H-1, δ 4.73–4.76 (42°C) and NAc, δ 2.015–2.019) (Hård *et al*., 1992; van Rooijen *et al*., 1998a,b), the Neu5Ac(α2–3)Gal element (Neu5Ac H-3a, δ 1.801 and H-3e, δ 2.754) (Hård *et al*., 1992), and the Neu5Ac(α2–6)Gal element (Neu5Ac H-3a, δ 1.719 and H-3e, δ 2.668) (Hård *et al*., 1992) are present.

Fraction **PIII** (Figure 4c). ^{1}H-NMR analysis of fraction **RCPIII** showed the presence of oligomannose-type glycans as the main components (Figure 5c) ($Man_5GlcNAc_2$: Man-**4** H-1, δ 5.097; $Man_6GlcNAc_2$: Man-**4** H-1, δ 5.344 and Man-**C** H-1, δ 5.050; $Man_7GlcNAc_2$: Man-**C** H-1, δ 5.307 and Man-$\mathbf{D_1}$ H-1, δ 5.041). This observation was supported by the HPAEC profile of **RCPIII** yielding 67% neutral oligosaccharides (Figures 6d, 7c) and 33% complex-type carbohydrate structures. Both peptide fractions **PIII9** and **PIII10** (Figure 4c) were subjected to N-terminal amino acid sequence analysis affording the partial sequences A-G-G-Y-Y- and PeC-A-G-G-Y-Y-V-Y-, respectively. As illustrated in Figure 2, the sequences of fractions **PIII9** and **PIII10** represent Ala244-Tyr248 and Cys243-Tyr250, respectively, meaning that both fractions were indicative for glycosylation site Asn251.

In order to investigate if the presence of oligomannose-type structures is restricted to only one glycosylation site in THp, fraction **P** (5 mg) was subjected to ConA Sepharose affinity chromatography (Figure 8a). Upon HPLC on ChromSpher 5 C8, fraction **P(CON-A)** released by elution with methyl α-D-mannopyranoside, comprised only one glycopeptide fraction (Figure 8b). After treatment of this fraction by PNGase-F, the digest was fractionated by HPLC on ChromSpher 5 C8 yielding subfraction **RCP(CON-A)** containing released glycans, and subfraction **P(CON-A)1** representing deglycosylated peptide material (Figure 8c). The deglycosylated peptide **P(CON-A)1** was subjected to

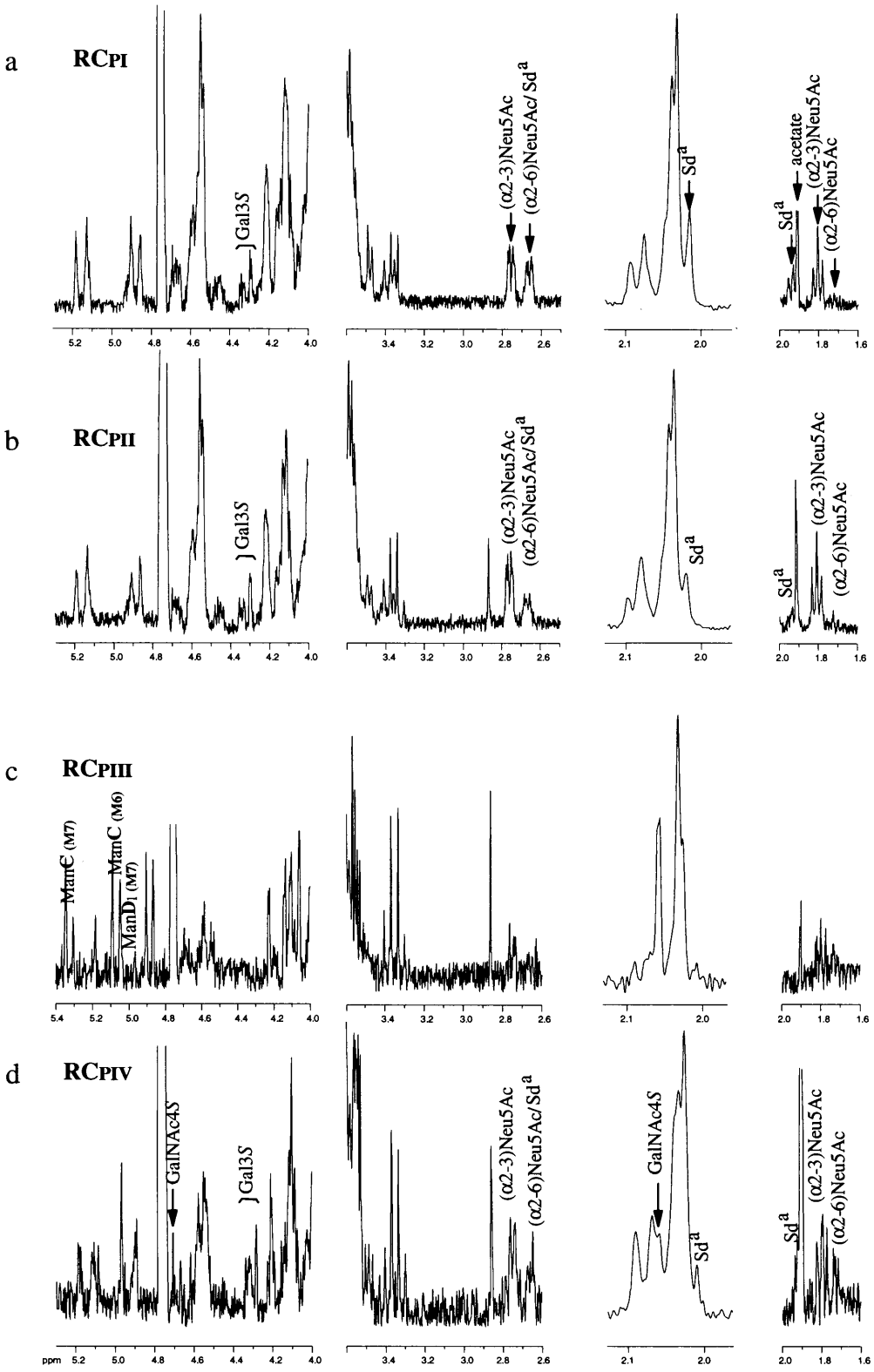

Fig. 5. Resolution-enhanced 500 MHz ^{1}H-NMR spectra at 300 K of fraction (**a**) **RCPI**, (**b**) **RCPII**, (**c**) **RCPIII**, and (**d**) **RCPIV**. Structural elements are displayed at the position of their structural-reporter-group signals (Hård *et al*., 1992; van Rooijen *et al*., 1998a,b).

N-terminal amino acid sequence analysis and fast atom bombardment mass spectrometry (FAB-MS). The N-terminal amino acid sequence analysis afforded the partial sequence PeC-A-G-G-Y-Y-V-Y-, corresponding with the sequence Cys243-Tyr250, being indicative of a glycosylated Asn251 residue (Figure 2). The FAB-mass spectrum of fraction **P(CON-A)1** contained two intense pseudomolecular ion pairs. The more intense of these, *m/z* 1282 $[M+H]^+$ and 1304 $[M+Na]^+$, corre-

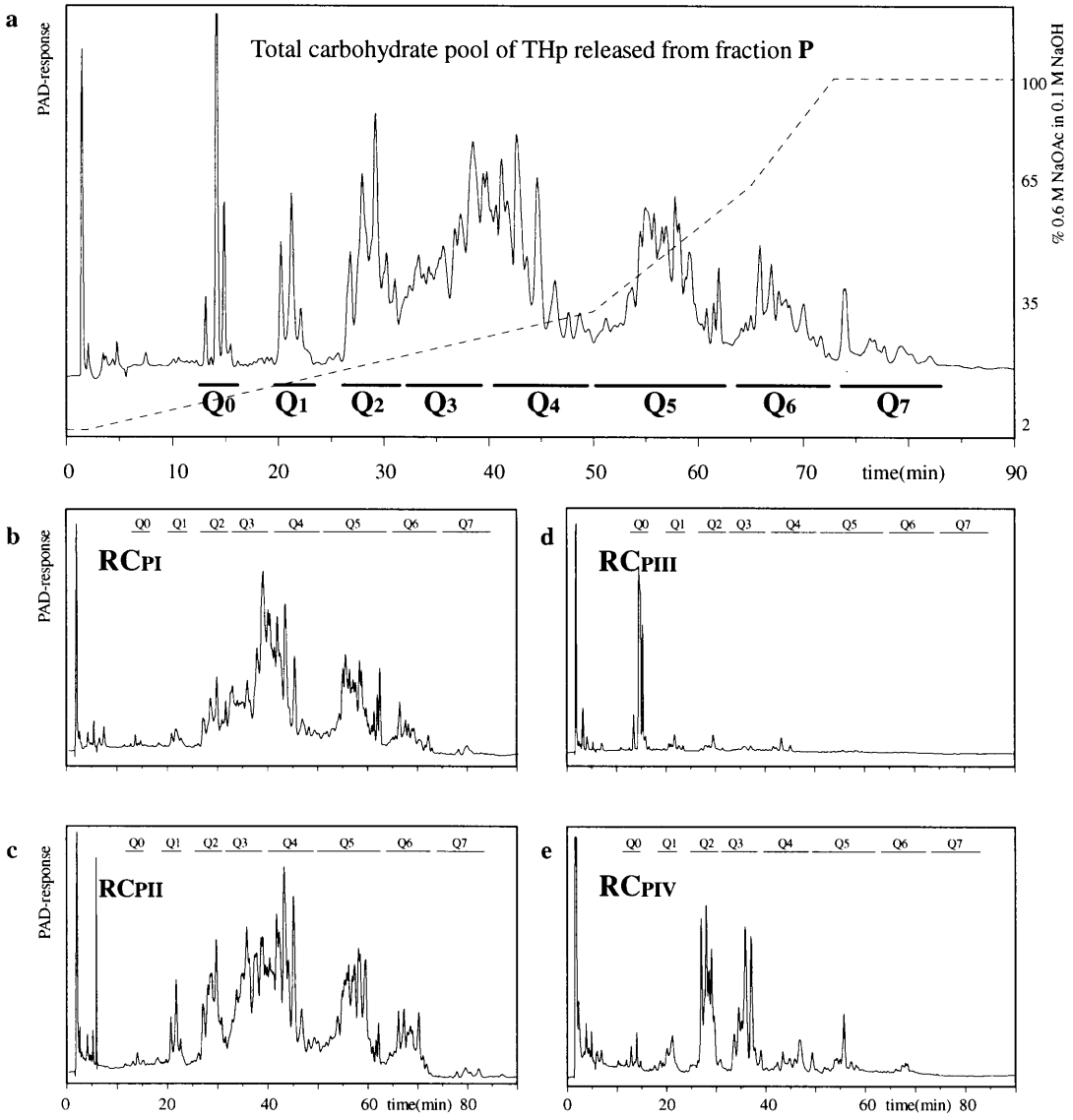

Fig. 6. HPAEC profiles of the released carbohydrate chains of the PNGase-F-treated glycopeptide fractions **PI-PIV** on CarboPac PA-100 with pulsed amperometric detection**.** Elutions were carried out on a CarboPac PA-100 column (4.6 × 250 mm, Dionex) with a concentration gradient of NaOAc in 0.1 M NaOH as indicated in (**a**), at a flow rate of 1 ml/min. The assignment of the regions differing in charge, charge fractions **Q0-Q7**, is based on a sequential Resource Q-CarboPac PA-100 approach (Hermentin *et al*., 1996). (**a**) total carbohydrate pool of **P**; (**b**) **RCPI**; (**c**) **RCPII**; (**d**) **RCPIII**; and (**e**) **RCPIV**.

sponds in mass to the carboxymethylated peptide Cys243-Thr253 in which the glycosylated Asn251 residue has been converted into Asp251 due to the action of PNGase-F. The less intense pair of ions at *m/z* 993 $[M+H]^+$ and 1015 $[M+Na]^+$ corresponds to peptide Gly246-Thr253, a breakdown product of the major component. HPAEC profiling of the glycan mixture in fraction **RCP(CON-A)** (Figure 9a) indicated the presence of 6% $Man_5GlcNAc_2$, 79% $Man_6GlcNAc_2$, 13% $Man_7GlcNAc_2$, and 2% $Man_8GlcNAc_2$ (reference compounds isolated from RNase-B, Figure 9b). ^{1}H-NMR analysis of fraction **RCP(CON-A)** confirmed the findings of $Man_5GlcNAc_2$, $Man_6GlcNAc_2$, and $Man_7GlcNAc_2$. In $Man_7GlcNAc_2$ Man-**C** is substituted with (α1–2)Man (Man-**C** H-1 at δ 5.307; van Kuik *et al*., 1992). Because of the low amount of material, $Man_8GlcNAc_2$ could not be confirmed by ^{1}H-NMR spectroscopy. Precise structures are given in Figure 9a. In conclusion, glycosylation site Asn251 contains predominantly oligomannose-type glycans, ranging from $Man_5GlcNAc_2$ to $Man_8GlcNAc_2$. Furthermore, this glycosylation site is the only one present in THp which contains oligomannose-type carbohydrate structures.

Fraction **PII** (Figure 4b). Peptide fractions **PII12**, **PII13**, and **PII14** were subjected to N-terminal amino acid sequence analysis yielding the overlapping partial sequences N-T-A-A-P-, A-A-P-M-W-L-, and R-C-N-T-A-, respectively. As is evident from Figure 2, these sequences represent Asn200-Pro204, Ala202-Leu207, and Arg198-Ala202, respectively, indicative of glycosylation site Asn208. The N-terminal amino acid sequence analysis of the minor fraction **PII11** (D-PeC-K-S-N-, Asp281-Asn285; Figure 2) is indicative of glycosylation site Asn298. The HPAEC profile of carbohydrate fraction **RCPII** (Figure 6c) shows the same microheterogeneity and ratio between the different charge fractions, as the HPAEC profile of the total carbohydrate moiety of THp (Figure 6a), except for the neutral carbohydrate chains (Figure 7b). ^{1}H-NMR analysis of fraction

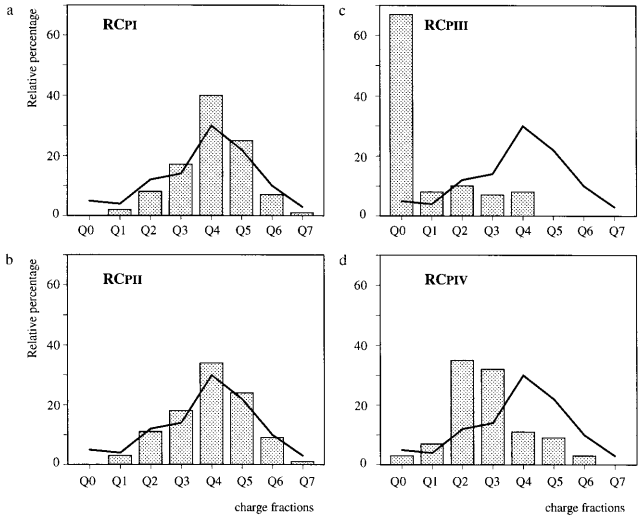

Fig. 7. The relative ratio (%) of charge fractions **Q0**-**Q7** calculated from the HPAEC profiles of the released carbohydrate chains of peptide fractions **PI**, **PII**, **PIII**, and **PIV** displayed in Figure 6. (**a**) **RCPI**; (**b**) **RCPII**; (**c**) **RCPIII**; (**d**) **RCPIV**. Plotted line represents the relative ratio (%) of charge fractions **Q0**-**Q7** of the total carbohydrate moiety obtained from PNGase-F-treated fraction **P**.

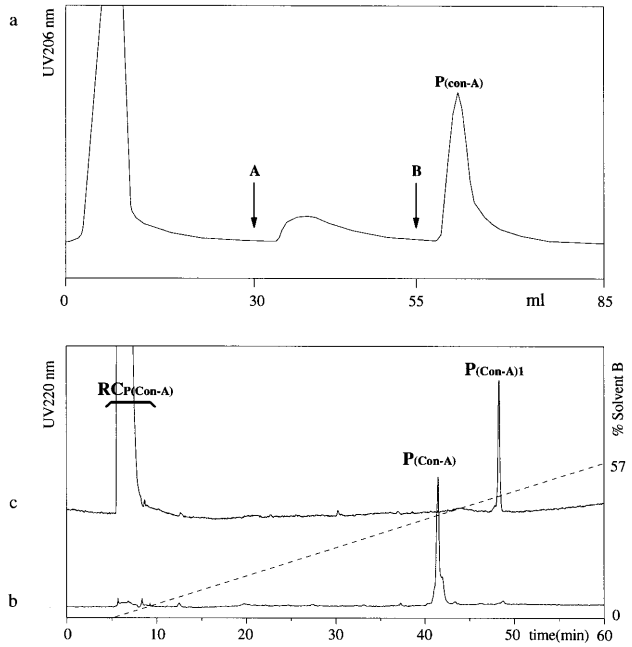

Fig. 8. (**a**) Elution profile at 206 nm on ConA-Sepharose (Pharmacia) of (glyco)peptide fraction **P**. The elution was started with 30 ml 20 mM Tris–HCl, pH 7.4, containing 0.5 M NaCl, 1 mM $CaCl_2$, and 1 mM $MgCl_2$ (Buffer A) at a flow rate of 15 ml/h. Then, elution of retained glycopeptides containing diantennary complex- and oligomannose-type oligosaccharides was performed by eluting with 25 ml 10 mM methyl α-D-glucopyranoside in buffer A at room temperature (start is indicated in the figure as **A**) and 30 ml 100 mM methyl α-D-mannopyranoside in buffer A at 60 °C (start is indicated in the figure as **B**), respectively. **P(CON-A)** represents the fraction released by methyl α-D-mannopyranoside. (**b**) Elution profile at 220 nm on ChromSpher 5 C8 of fraction **P(CON-A)**. Conditions are described in Figure 3. (**c**) Elution profile at 220 nm on ChromSpher 5 C8 of PNGase-F–treated fraction **P(CON-A)**. **RCP(CON-A)** contains the liberated oligosaccharides from the deglycosylated peptide **P(CON-A)1**. Conditions are described in Figure 3.

RCPII (Figure 5b) showed the presence of Gal3*S* residues, the Sd^a-determinant, the Neu5Ac(α2–3)Gal element, and the Neu5Ac(α2–6)Gal element. In view of the relatively low amount of peptide **PII11**, correlated with Asn298, it can be concluded that the carbohydrate chains released from glycopeptide fraction **PII** mainly resemble the site-specific glycosylation of Asn208.

Fraction **PI** (Figure 4a). N-Terminal amino acid sequence analysis of peptide fraction **PI2** showed the partial sequence N-PeC-Y-A-T-P-, which corresponds with Asn481-Pro486 (Figure 2), therefore being indicative of glycosylation site Asn489. The peptide in fraction **PI3** reflects glycosylation site Asn372, as can be deduced from the N-terminal amino acid sequence analysis demonstrating the sequence G-P-PeC-G-T-, corresponding with Gly363-Thr367 (Figure 2). Subjection of fraction **PI4** to N-terminal amino acid sequence analysis afforded the partial sequence H-PeC-Q-PeC-K-, corresponding with the sequence His290-Lys294. This is indicative of a peptide containing glycosylated Asn298. N-Terminal amino acid sequence analysis of fractions **PI5**, **PI6**, and **PI7** revealed partial sequences of peptides containing glycosylation sites Asn52 and Asn56 (**PI5**: PeC-A-I-P-G-A-H-D-C-S-A-D-S-, Cys45-Ser57; **PI6**: PeC-A-I-P-G-, Cys45-Gly49; **PI7**: PeC-A-I-P-G-, Cys45-Gly49). Both Asn52 and Asn56 are glycosylated as follows from the partial sequence of the peptide in fraction **PI5**, wherein Asn52 and Asn56 occur as Asp52 and Asp56, respectively. ^{1}H-NMR analysis of the oligosaccharide fraction **RCPI** showed the presence of Gal3*S* residues, the Sd^a-determinant, Neu5Ac(α2–3)Gal elements, and Neu5Ac(α2–6)Gal elements. The HPAEC profile of carbohydrate fraction **RCPI** (Figure 6b) reflects a large microheterogeneity and the ratio of the different charge fractions is similar to that found for the total carbohydrate moiety of THp (Figure 7a), except for the neutral carbohydrate chains. Note that the oligosaccharides found in fraction **PI** represent the total carbohydrate pattern of five glycosylation sites (Asn52, Asn56, Asn298, Asn 372, and Asn489).

Discussion

Tamm-Horsfall glycoprotein has previously been shown to contain eight potential glycosylation sites (Hession *et al*., 1987; Pennica *et al*., 1987), of which at least five were glycosylated (Afonso *et al*., 1981). In this study, we characterized the glycosylation sites of THp from one healthy male donor by analysis of glycopeptides formed by proteolysis by V-8 protease. In some cases, more than one glycopeptide was generated representing the same glycosylation site. Out of the eight potential glycosylation sites, seven are occupied, namely, Asn52, Asn56, Asn208, Asn251, Asn298, Asn372, and Asn489 (Figure 10). The potential glycosylation site at Asn14, being close to the N-terminus, is not used. Here, also the microheterogeneity of the glycosylation sites Asn489, Asn251, and Asn208 has been analyzed in more detail.

It should be noted that in view of the complexity of the structural studies of THp, so far no quantitative data with respect to the level of site-occupancy of the seven Asn residues has been generated.

Glycans at Asn489 can be terminated by GalNAc4*S*(β1–4)GlcNAc and mainly di- and tri-charged N-glycans are observed. These findings are in agreement with the observation that the GalNAc4*S*(β1–4)GlcNAc structural element is only established yet for diantennary N-glycans of THp (compounds

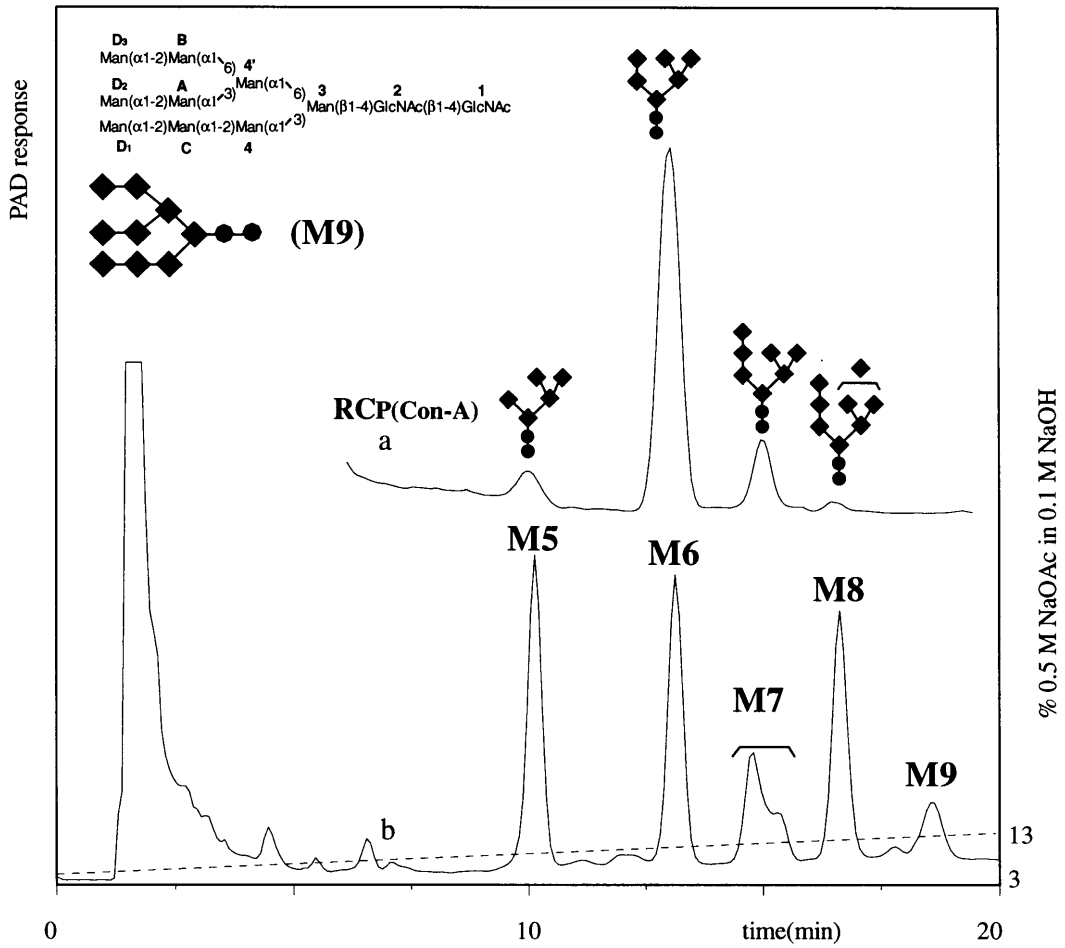

Fig. 9. HPAEC profiles of oligomannose-type carbohydrate chains on CarboPac PA-100 with pulsed amperometric detection. (**a**) Fraction **RCP(CON-A)**, containing the released oligosaccharides of the PNGase-F-treated glycopeptide fraction **P(CON-A)**. (**b**) Oligomannose-type structures of RNase-B. **M5** to **M9** represent oligomannose-type structures $Man_5GlcNAc_2$ to $Man_9GlcNAc_2$, respectively. Compounds are represented by shorthand symbolic notation: solid diamonds, Man; solid circles, GlcNAc. For $Man_9GlcNAc_2$ the numbering of the individual monosaccharide residues is given. Elutions were performed as indicated in the figure.

N3.2.1 and **N3.2.3** in Hård *et al*., 1992; compounds **Q3.1.1**, **Q3.1.3**, **Q3.1.5** and **Q3.1.11B** in van Rooijen *et al*., 1998b), although evidence was found for GalNAc4*S*-containing triantennary compounds as well (van Rooijen *et al*., 1998b). Other urinary glycoproteins, like urokinase (Bergwerff *et al*., 1995) and kallidinogenase (Tomiya *et al*., 1993), also display the GalNAc(β1–4)GlcNAc element. In the case of urokinase also 4-*O*-sulfated GalNAc occurs. Interestingly, it should be noticed that the GalNAc4*S*(β1–4)GlcNAc structural element seems to occur exclusively at Asn489 with a Pro-Leu-Lys peptide motif, located 3 residues on the COOH-terminal side. So far, it has been suggested that the sequon Pro-Xaa-Arg/Lys at the NH_2-terminal side at various positions is responsible for directing the specificity of the β4-GalNAc-transferase (Smith and Baenziger, 1992; Sato *et al*., 1995). Since such a sequon is located now also at the COOH-terminal direction of the Asn glycosylation site, it may be rather the influence of the three-dimensional structure of the protein near the glycosylation site that is responsible than a sequon.

Only glycosylation site Asn251 contains oligomannose-type structures (5% of the total carbohydrate pool based on the ratios on CarboPac PA-100, Figure 6a) ranging from $Man_5GlcNAc_2$ to $Man_8GlcNAc_2$. Besides these oligomannose-type carbohydrate chains (67%), glycosylation site Asn251 contains 33% of complex-type N-glycans. The molar ratio of 6:79:13 for $Man_5GlcNAc_2$:$Man_6GlcNAc_2$:$Man_7GlcNAc_2$ is in agreement with reference data (Dall'Olio *et al*., 1988). However, we demonstrated the additional presence of $Man_8GlcNAc_2$ in a low amount (in the molar ratio of 2). In earlier studies THp has shown to contain 20% (Smagula *et al*., 1990; Serafini-Cessi *et al*., 1984a; based on peak heights), 16% (Dall'Olio *et al*., 1988), 2% (Afonso *et al*., 1981), and 0% (Hård *et al*., 1992) oligomannose-type carbohydrate chains. The level of oligomannose-type carbohydrate chains is therefore possibly a donor-specific feature. It should be noted that oligomannose-type carbohydrate chains are supposed to play a predominant role in the immunosuppressive properties displayed by THp (Serafini-Cessi *et al*., 1979; Muchmore *et al*., 1987, 1990a,b; Moonen *et al*., 1988; Smagula *et al*., 1990).

Finally, glycosylation site Asn208 shows a large microheterogeneity resembling that of the total glycan pool of THp (Figures 7a and 7c).

The detailed knowledge of the glycosylation pattern of THp including the donor-specificity (Hård *et al*., 1992; van Rooijen *et al*., 1998a,b; this study), makes further studies with respect to the biological significance of THp challenging.

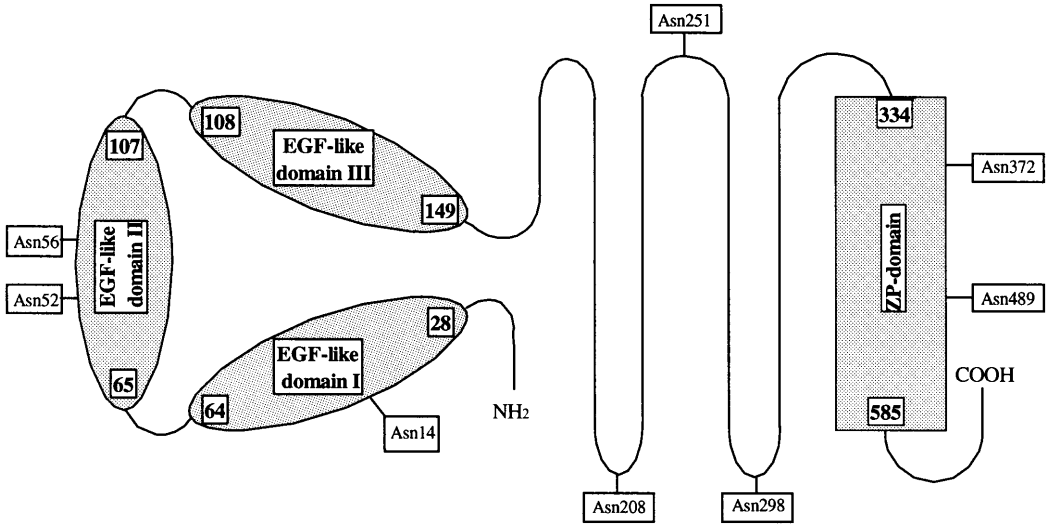

Fig. 10. Schematic representation of THp including its specific domains and potential glycosylation sites. THp contains eight potential glycosylation sites, but only Asn14 is not glycosylated. Three EGF-like domains and one ZP-domain are present (Hession *et al*., 1987; Pennica *et al*., 1987; SWISS-PROT Database, id. p07911) as indicated in the figure. EGF-like domain, epidermal growth factor-like domain; ZP-domain, zona pellucida domain.

Material and methods

Materials

THp was isolated from pooled morning urine of a healthy male donor as described previously (Serafini-Cessi *et al*., 1989). Recombinant peptide-N^4-(*N*-acetyl-β-glucosaminyl)asparagine amidase F (PNGase-F) from *Flavobacterium meningosepticum* (EC 3.5.1.52) and endoproteinase Glu-C (V-8 protease, EC 3.4.21.1g) from *Staphylococcus aureus* were purchased from Boehringer Mannheim, Germany.

Reduction and S-carboxymethylation

THp was reduced and *S*-carboxymethylated using standard methods (Lustbader *et al*., 1989). Briefly, THp (75 mg) was dissolved in 20 ml 1 M Tris–HCl, pH 8.25, containing 6 M guanidine-HCl, 1 mM EDTA and 50 mM DTT, and the mixture was incubated for 2 h at 37°C. After cooling down to room temperature, iodoacetic acid (0.5 M in 0.5 M NaOH) was added to a final concentration of 100 mM, and the mixture was incubated in the dark for 30 min. The reaction was quenched by adding an excess of β-mercaptoethanol. Salts were removed by dialyzing the sample three times against water. Next, the THp solution was lyophilized and stored at -20°C prior to use. The purity was checked by SDS–PAGE under reducing and nonreducing conditions.

Endoproteinase Glu-C digestion

Reduced and carboxymethylated THp (50 mg) was dissolved in 15 ml 50 mM phosphate buffer, pH 7.8, and incubated with endoproteinase Glu-C (1 mg) at 37°C. After 18 h, a second portion of endoproteinase Glu-C (1 mg) was added and the digestion was continued for 18 h at 37°C. After lyophilization, the digest was fractionated on four connected HiTrap columns (4 × 5 ml, Pharmacia) using 5 mM NH_4HCO_3, pH 7.0, as eluent at a flow rate of 4 ml/min. The effluent was monitored at 278 nm and the void-volume fraction, containing the glycopeptides (orcinol/H_2SO_4 assay), was isolated and lyophilized.

Affinity chromatography

An aliquot of the glycopeptide mixture (5 mg) was applied to a Concanavalin A Sepharose column (2 ml, Pharmacia) and first eluted with 30 ml 20 mM Tris–HCl, pH 7.4, containing 0.5 M NaCl, 1 mM $CaCl_2$, and 1 mM $MgCl_2$ (buffer A) at a flow rate of 15 ml/h. Then the elution was continued with 25 ml 10 mM methyl α-D-glucopyranoside in buffer A at room temperature to desorb diantennary-complex-type glycopeptides, and finally with 30 ml 100 mM methyl α-D-mannopyranoside in buffer A at 60°C to desorb oligomannose-type glycopeptides. All fractions were lyophilized, desalted by HiTrap (Pharmacia FPLC system; four columns connected, 4 × 5 ml; eluent, 5 mM NH_4HCO_3; flow rate, 3 ml/min; detection, 206 nm), and lyophilized again. Glycopeptides containing oligomannose-type structures were fractionated by HPLC as described below.

HPLC

(Glyco)peptide mixtures were fractionated by HPLC on a ChromSpher 5 C8 column (10×250 mm, Chrompack) at a flow rate of 2.5 ml/min, using a Kratos SF 400 HPLC system (ABI Analytical, Kratos Division). The column was eluted isocratically with solvent A (aqueous 5% acetonitrile containing 0.1% trifluoroacetic acid) for 5 min, followed by a linear concentration gradient from 100% solvent A/0% solvent B (aqueous 80% acetonitrile containing 0.1% trifluoroacetic acid) to 43% solvent A/57% solvent B in 55 min. The effluent was monitored at 220 nm using a Spectroflow 757 absorbance detector (ABI Analytical, Kratos Division). Fractions were collected manually and immediately dried in a SpeedVac and lyophilized. Fractions containing glycopeptides were detected using orcinol/H_2SO_4.

Liberation of the N-linked carbohydrate chains from glycopeptides

Glycopeptide mixtures were dissolved in 100 µl 50 mM phosphate buffer, pH 8.2, containing 10 mM EDTA, then incubated with 0.5 U PNGase-F at 37°C. After 18 h, the digest was boiled for 3 min and cooled down to room temperature. In each case the digest was fractionated by HPLC as described

above. The HPLC-void-volume fraction, containing the liberated carbohydrate chains, was desalted by HiTrap (Pharmacia), and lyophilized. The fractions containing deglycosylated peptides were immediately dried in a SpeedVac, lyophilized, and subsequently analyzed for their N-terminal amino acid sequence.

Oligosaccharide profiling on HPAEC

Each HPLC-void-volume fraction, stemming from PNGase-F–treated glycopeptides, was analyzed for oligosaccharide components by HPAEC, using a Dionex DX500 chromatography system, equipped with a CarboPac PA-100 column (4.6 × 250 mm, Dionex) (Hermentin *et al*., 1992). Oligosaccharides were separated using a concentration gradient of NaOAc in 0.1 M NaOH as indicated in the figures, at a flow rate of 1 ml/min. Pulsed amperometric detection was performed using the following pulse potentials and durations: E_1 = 0.05 V (400 ms); E_2 = 0.75 V (200 ms); E_3 = -0.15 V (400 ms).

^{1}H-NMR spectroscopy

Prior to ^{1}H-NMR analysis, samples were exchanged twice in 99.9% ^2H_2O with intermediate lyophilization and finally dissolved in 450 µl 99.96% ^2H_2O (Isotec Inc). 500 MHz ^{1}H-NMR spectra were recorded on a Bruker AMX-500 spectrometer (Bijvoet Center, Department of NMR Spectroscopy, Utrecht University) essentially as described previously (Hård *et al*., 1992).

Fast atom bombardment mass spectrometry

Positive-ion fast atom bombardment mass spectrometry (FAB-MS) of a deglycosylated peptide sample was performed using MS1 of a JEOL JMS-SX/SX102A tandem mass spectrometer (Bijvoet Center, Department of Mass Spectrometry, Utrecht University), using 10 kV accelerating voltage. The FAB gun was operated at an emission current of 10 mA, with Xe as bombarding gas. The spectra were scanned at a speed of 30 s for full mass range specified by the accelerating voltage used, and were recorded and averaged on a Hewlett Packard HP9000 data system. Samples were dissolved in 10 µl aqueous 5% HOAc and 1 µl was loaded into a matrix of thioglycerol.

Acknowledgments

We are grateful to Dr. J. Thomas-Oates (Bijvoet Center, Department of Mass Spectroscopy) for recording and interpreting the FAB-mass spectrum. This work was supported by the Netherlands Foundation for Chemical Research (S.O.N.) with financial aid from the Netherlands Organization for Scientific Research (N.W.O.).

References

Afonso,A.-M.M., Charlwood,P.A. and Marshall,R.D. (1981) Isolation and characterisation of glycopeptides from digests of human Tamm-Horsfall glycoprotein. *Carbohydr. Res*., **89,** 309–319.

Bergwerff,A.A., van Oostrum,J., Kamerling,J.P. and Vliegenthart,J.F.G. (1995) The major N-linked carbohydrate chains from human urokinase. The occurrence of 4-*O*-sulfated, (α2–6)-sialylated or (α1–3)-fucosylated *N*-acetylgalactosamine(β1–4)-*N*-acetylglucosamine elements. *Eur. J. Biochem*., **228,** 1009–1019.

Dall'Olio,F., de Kanter,F.J.J., van den Eijnden,D.H. and Serafini-Cessi,F. (1988) Structural analysis of the preponderant high-mannose oligosaccharides of human Tamm-Horsfall glycoprotein. *Carbohydr. Res*., **178,** 327–332.

Donald,A.S.R. and Feeney,J. (1986) Oligosaccharides obtained from a blood-group-Sd(a+) Tamm-Horsfall glycoprotein: an n.m.r. study. *Biochem. J*., **236,** 821–828.

Donald,A.S.R., Yates,A.D., Soh,C.P.C., Morgan,W.T.J. and Watkins,W.M. (1983) A blood group Sd^a-active pentasaccharide isolated from Tamm-Horsfall urinary glycoprotein. *Biochem. Biophys. Res. Commun*., **115**, 625–631.

Duncan,J.L. (1988) Differential effect of Tamm-Horsfall protein on adherence of *Escherichia coli* to transitional epithelial cells. *J. Infect. Dis*., **158,** 1379–1382.

Hallson,P.C. and Rose,G.A. (1979) Uromucoids and urinary stone formation. *Lancet*, **1,** 1000–1002.

Hård,K., van Zadelhoff,G., Moonen,P., Kamerling,J.P. and Vliegenthart,J.F.G. (1992) The Asn-linked carbohydrate chains of human Tamm-Horsfall glycoprotein of one male. Novel sulfated and novel *N*-acetylgalactosamine-containing N-linked carbohydrate chains. *Eur. J. Biochem*., **209,** 895–915.

Hermentin,P., Witzel,R., Vliegenthart,J.F.G., Kamerling,J.P., Nimtz,M. and Conradt,H.S. (1992) A strategy for the mapping of N-glycans by high-pH anion-exchange chromatography with pulsed amperometric detection. *Anal. Biochem*., **203,** 281–289.

Hermentin,P., Witzel,R., Kanzy,E.-J., Diderrich,G., Hoffmann,D., Metzner,H., Vorlop,J. and Haupt,H. (1996) The hypothetical N-glycan charge: a number that characterizes protein glycosylation. *Glycobiology*, **6,** 217–230.

Hession,C., Decker,J.M., Sherblom,A.P., Kumar,S., Yue,C.C., Mattaliano,R.J., Tizard,R., Kawashima,E., Schmeissner,U., Heletky,S., Chow,E.P., Burne,C.A., Shaw,A. and Muchmore,A.V. (1987) Uromodulin (Tamm-Horsfall glycoprotein): a renal ligand for lymphokines. *Science*, **237,** 1479–1484.

Kamerling,J.P., Rijkse,I., Maas,A.A.M., van Kuik,J.A. and Vliegenthart,J.F.G. (1988) Sulfated N-linked carbohydrate chains in porcine thyroglobulin. *FEBS Lett*., **241,** 246–250.

Kumar,S. and Muchmore,A.V. (1990) Tamm-Horsfall protein-uromodulin (1950–1990). *Kidney Int*., **37,** 1395–1401.

Lustbader,J.W., Birken,S., Pileggi,N.F., Kolks,M.A., Pollak,S., Cuff,M.E., Yang,W., Hendrickson,K. and Canfield,R.E. (1989) Crystallization and characterization of human chorionic gonadotropin in chemically deglycosylated and enzymatically desialylated states. *Biochemistry*, **28,** 9239–9243.

Mattey,M. and Naftalin,L. (1992) Mechanoelectrical transduction, ion movement and water stasis in uromodulin. *Experientia*, **48,** 975–980.

Moonen,P., Gaffner,R. and Wingfield,P. (1988) Native cytokines do not bind to uromodulin (Tamm-Horsfall glycoprotein). *FEBS Lett*., **226,** 314–318.

Muchmore,A.V., Shifrin,S. and Decker,J.M. (1987) *In vitro* evidence that carbohydrate moieties derived from uromodulin, an 85,000 dalton immunosuppressive glycoprotein isolated from human pregnancy urine, are immunosuppressive in the absence of intact protein. *J. Immunol*., **138,** 2547–2553.

Muchmore,A.V., Decker,J.M., Shaw,A. and Wingfield,P. (1990a) Evidence that high-mannose glycopeptides are able to functionally interact with recombinant tumor necrosis factor and recombinant interleukin-1. *Cancer Res*., **50,** 6285–6290.

Muchmore,A.V., Sathyamoorthy,N., Decker,J.M. and Sherblom,A.P. (1990b) Evidence that specific high-mannose oligosaccharides can directly inhibit antigen-driven T-cell responses. *J. Leukoc. Biol*., **48,** 457–464.

Parkkinen,J., Virkola,R. and Korhonen,T.K. (1988) Identification of factors in human urine that inhibit the binding of *Escherichia coli* adhesins. *Infect. Immun*., **56,** 2623–2630.

Pennica,D., Kohr,W.J., Kuang,W.-J., Glaister,D., Aggarwal,B.B., Chen,E.Y. and Goeddel,D.V. (1987) Identification of human uromodulin as the Tamm-Horsfall urinary glycoprotein. *Science*, **236,** 83–88.

Rindler,M.J., Naik,S.S., Li,N., Hoops,T.C. and Peraldi,M.N. (1990) Uromodulin (Tamm-Horsfall glycoprotein/uromucoid) is a phosphatidylinositol-linked membrane protein. *J. Biol. Chem*., **265,** 20784–20789.

Sathyamoorthy,N., Decker,J.M., Sherblom,A.P. and Muchmore,A.V. (1991) Evidence that specific high mannose structures directly regulate multiple cellular activities. *Mol. Cell Biochem*., **102,** 139–147.

Sato,T., Takio,K., Kobata,A., Greenwalt,D.E. and Furukawa,K. (1995) Site-specific glycosylation of bovine butyrophilin. *J. Biochem. (Tokyo)*, **117,** 147–157.

Scurr,D.S. and Robertson,W.G. (1986) Modifiers of calcium oxalate crystallisation found in urine. III. Studies on the role of Tamm-Horsfall mucoprotein and of ionic strenght. *J. Urol*., **136,** 505–507.

Serafini-Cessi,F., Franceschi,C. and Sperti,S. (1979) Specific interaction of human Tamm-Horsfall glycoprotein with leucoagglutinin, a lectin from *Phaseolus vulgaris* (red kidney bean). *Biochem. J*., **183,** 381–388.

Serafini-Cessi,F., Dall'Olio,F. and Malagolini,N. (1984a) High-mannose oligosaccharides from human Tamm-Horsfall glycoprotein. *Biosci. Rep*., **4,** 269–274.

Serafini-Cessi,F., Malagolini,N. and Dall'Olio,F. (1984b) A tetraantennary glycopeptide from human Tamm-Horsfall glycoprotein inhibits agglutination of desialylated erythocytes induced by leucoagglutinin. *Biosci. Rep*., **4,** 973–978.

Serafini-Cessi,F., Bellabarba,G., Malagolini,N. and Dall'Olio,F. (1989) Rapid isolation of Tamm-Horsfall glycoprotein (uromodulin) from human urine. *J. Immunol. Methods*, **120,** 185–189.

Sikri,K.L., Foster,C.L., Bloomfield,F.J. and Marshall,R.D. (1979) Localization by immunofluorescence and by light- and electron-microscopic immunoperoxidase techniques of Tamm-Horsfall glycoprotein in adult hamster kidney. *Biochem. J*., **181,** 525–532.

Smagula,R.M., van Halbeek,H., Decker,J.M., Muchmore,A.V., Moody,C.E. and Sherblom,A.P. (1990) Pregnancy-associated changes in oligomannose oligosaccharides of human and bovine uromodulin (Tamm-Horsfall glycoprotein). *Glycoconjugate J*., **7,** 609–624.

Smith,P.L. and Baenziger,J.U. (1992) Molecular basis of recognition by the glycoprotein hormone specific *N*-acetylgalactosamine-transferase. *Proc. Natl. Acad. Sci. USA*, **89,** 329–333.

Tamm,I. and Horsfall,F.L. (1950) Characterization and separation of an inhibitor of viral hemagglutination present in urine. *Proc. Soc. Exp. Biol. Med*., **74,** 108–114.

Tamm,I. and Horsfall,F.L. (1952) A mucoprotein derived from human urine which reacts with influenza, mumps, and Newcastle disease viruses. *J. Exp. Med*., **95,** 71–79.

Toma,G., Bates,J.M. and Kumar,S. (1994) Uromodulin (Tamm-Horsfall protein) is a leukocyte adhesion molecule. *Biochem. Biophys. Res. Commun*., **200,** 275–282.

Tomiya,N., Awaya,J., Kurono,M., Hanzawa,H., Shimada,I., Arata,Y., Yoshida,T. and Takahashi,N. (1993) Structural elucidation of a variety of GalNAc-containing N-linked oligosaccharides from human urinary kallidinogenase. *J. Biol. Chem*., **268,** 113–126.

Van Kuik,J.A., Hård,K. and Vliegenthart,J.F.G. (1992) A ^{1}H NMR database computer program for the analysis of the primary structure of complex carbohydrates. *Carbohydr. Res*., **235,** 53–68.

van Rooijen,J.J.M., Kamerling,J.P. andVliegenthart,J.F.G (1998a) The abundance of additional *N*-acetyllactosamine units in N-linked tetraantennary oligosaccharides of human Tamm-Horsfall glycoprotein is a donor-specific feature. *Glycobiology*, **8,** 1065–1075.

van Rooijen,J.J.M., Kamerling,J.P. and Vliegenthart,J.F.G. (1998b) Sulfated di-, tri- and tetraantennary N-glycans in human Tamm-Horsfall glycoprotein. *Eur. J. Biochem.*, **256,** 471–487.

Williams,J., Marshall,R.D., van Halbeek,H. and Vliegenthart,J.F.G. (1984) Structural analysis of the carbohydrate moieties of human Tamm-Horsfall glycoprotein. *Carbohydr. Res*., **134**, 141–155.